**Author(s):** Ojajärvi, Risto; Heikkilä, Tero T.; Virtanen, P.; Silaev, M. A.

**Title:** Giant enhancement to spin battery effect in superconductor/ferromagnetic insulator systems

**Year:** 2021

**Version:** Published version

# Giant enhancement to spin battery effect in superconductor/ferromagnetic insulator systems

Risto Ojajärvi,[1] Tero T. Heikkilä,[1] P. Virtanen,[1] and M. A. Silaev[1,2,3]
[1]*Department of Physics and Nanoscience Center, University of Jyväskylä, P.O. Box 35 (YFL), FI-40014 University of Jyväskylä, Finland*
[2]*Moscow Institute of Physics and Technology, 141700 Dolgoprudny, Russia*
[3]*Institute for Physics of Microstructures, Russian Academy of Sciences, 603950 Nizhny Novgorod, GSP-105, Russia*

(Received 15 March 2021; accepted 3 June 2021; published 22 June 2021)

We develop a theory of the spin battery effect in superconductor/ferromagnetic insulator (SC/FI) systems taking into account the magnetic proximity effect. We demonstrate that the spin-energy mixing enabled by the superconductivity leads to the enhancement of spin accumulation by several orders of magnitude relative to the normal state. This finding can explain the recently observed giant inverse spin Hall effect generated by thermal magnons in the SC/FI system. We suggest a nonlocal electrical detection scheme which can directly probe the spin accumulation driven by the magnetization dynamics. We predict a giant Seebeck effect converting the magnon temperature bias into the nonlocal voltage signal. We also show how this can be used to enhance the sensitivity of magnon detection even up to the single-magnon level.

DOI: 10.1103/PhysRevB.103.224524

Generation and detection of pure spin signals is one of the main paradigms in spintronics [1,2] and spin caloritronics [3]. Spin pumping [4–6] in ferromagnet/metal multilayers affects ferromagnetic resonance (FMR) and spin Hall magnetoresistance measurements [7,8]. Spin Seebeck effect [8,9] converts thermal nonequilibrium states into pure spin currents and can be used for the detection of magnons propagating through FI materials without electrical losses [10,11]. Pure spin current flowing from the ferromagnet into the adjacent metal leads to the buildup of spin accumulation known as the spin battery effect [5].

Recently it has been discovered [12–17] that superconductivity strongly increases spin relaxation times and lengths, which makes superconducting materials promising for spintronics [18–20]. Long-range nonequilibrium spin states created in superconductors by electrical and thermal injection of Bogoliubov quasiparticles have been intensively studied [20–28]. The question of how the weak spin relaxation in superconductors shows up in spin pumping properties have remained unexplored and is addressed in the present paper.

Most of the experimental [13,15,16,29–34] and theoretical works studying magnetization dynamics in superconductor/ferromagnet systems focus on the FMR properties [35–41] and spin torques [42,43]. Here we consider the spin battery effect [5] that is the static spin accumulation of Bogoliubov quasiparticles in a superconductor (SC) generated either by the coherent FMR drive or by the thermal magnons in the adjacent FI. Our study is motivated by the recent experiment demonstrating that magnons induce a giant inverse spin-Hall signal in the transition state of the Nb/YIG superconductor/ferromagnetic insulator system [34]. Due to the close relation between the spin Hall signal and spin density, this observation hints that the spin accumulation induced by thermal magnons is modified in a highly nontrivial way by the superconducting correlations.

The considered setup is detailed in Fig. 1(a) which shows the time-averaged quasiparticle spin accumulation $\langle \boldsymbol{\mu}_s \rangle$ generated in SC. It can be measured [12,13,15,16] in the nonlocal circuit Fig. 1(b) consisting of the spin-polarized tunnel contact with a metallic ferromagnet (FM) near FI and the distant normal metal electrode (NM). The dc voltage $V_D$ induced into this tunnel contact in the absence of a charge current through it is [23]

$$V_D = \frac{G_{Fn}}{G_F} \boldsymbol{P}_D \cdot \langle \boldsymbol{\mu}_s \rangle. \tag{1}$$

Here $G_F = G_{Fn} \int_0^\infty d\varepsilon N(\varepsilon) \partial_\varepsilon n_0$ is the linear local tunneling conductance and $\boldsymbol{P}_D$ the spin polarization of the SC/FM junction, $N(\varepsilon)$ is the density of states in the superconductor, and $n_0 = \tanh(\varepsilon/2T)$ is the equilibrium distribution function.

In the superconducting case the information carried by the strength of the spin pumping which determines the FMR linewidth is different from that in $\langle \boldsymbol{\mu}_s \rangle$. It is generally proportional to the amplitude of magnetization dynamics $\langle \boldsymbol{\mu}_s \rangle \propto \langle \boldsymbol{m} \times \partial_t \boldsymbol{m} \rangle$, where $\boldsymbol{m}(t)$ is the unit vector of magnetization direction in FI. In superconductors, however, the proportionality constant of $\langle \boldsymbol{\mu}_s \rangle$ is sensitive to the magnitude of energy relaxation time $\Gamma^{-1}$ and its magnitude compared to the spin-relaxation time $\tau_s$. In the typical case $\Gamma^{-1} \gg \tau_s$ the resulting nonlocal voltage $V_D$ can be parametrically larger in the superconducting state than in the normal state by the factor $\sim(\Gamma\tau_s)^{-1}$. In superconductors Nb and Al these times are of the order [15,44] of $\tau_s \approx 0.1 T_c^{-1}$ in Al and and $\tau_s \approx T_c^{-1}$ in Nb, while $\Gamma^{-1}(T_c) \approx 10^3 T_c^{-1}$ in both materials [45,46]. Therefore in these superconductors one can expect an enhancement of spin accumulation induced by spin pumping by the factor of $(\Gamma\tau_s)^{-1} \sim 10^2$–$10^3$ as compared to the normal state.

The origin of the very large spin accumulation in FI/SC contacts is twofold. First, magnetization dynamics results

 

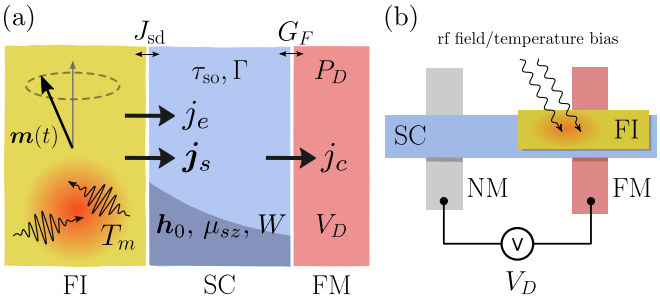


FIG. 1. Schematic FI/SC setup to measure spin accumulation induced by magnons. (a) Nonequilibrium magnon distribution in FI, generated either by a coherent FMR drive or a temperature bias, induces spin and energy currents $\boldsymbol{j}_s$ and $j_e$ to the SC, which create spin and energy accumulations $\boldsymbol{\mu}_s$ and $W$ in SC. Proximity to FI also induces a static exchange field $\boldsymbol{h}_0$ in the SC. The spin accumulation is converted to electrical voltage $V_D$ in the ferromagnetic electrode (FM) with the polarization $P_D$. (b) Nonlocal circuit to measure magnon-induced voltage $V_D$.

in the energy current [4,47] $j_e = \alpha\langle|\partial_t \boldsymbol{m}|^2\rangle$, where $\alpha$ is the contribution to the Gilbert damping coefficient due to the contact. Second, in superconductors the spin splitting in the Bogoliubov spectrum generated by FI through the magnetic proximity effect [20,23,48,49] leads to the strong coupling between energy and spin degrees of freedom [23]. The mechanism of converting pumped quasiparticle energy to spin accumulation via elastic spin-relaxation processes is demonstrated in Fig. 2 which shows nonequilibrium quasiparticle states on the spin-split Bogoliubov branches $E_p(p)$ for different momenta $p$. The spin quantization axis is determined by the Zeeman field $\boldsymbol{h}_0 = h_0\boldsymbol{z}$ induced by the *magnetic proximity effect*, when the static magnetization direction is $\boldsymbol{m}_0 = \boldsymbol{z}$.

Energy current $j_e$ generates spin-neutral energy accumulation $W$ by nonequilibrium quasiparticle states shown schematically by the filled circles in Fig. 2(a). The important feature of this distribution is that both spin-up and spin-down branches have the same number of occupied states. Due to the spin splitting the spin-up and spin-down branches are filled up

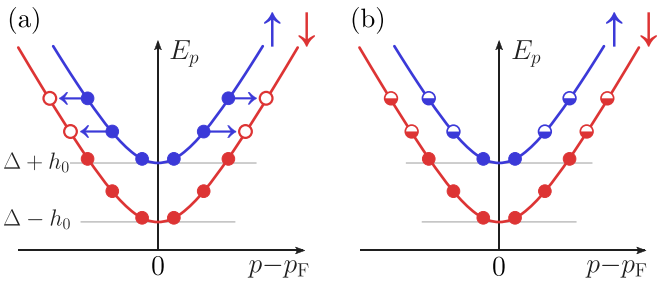


FIG. 2. Spin-split Bogoliubov spectrum in SC and its occupation driven by magnons. (a) State with pure energy accumulation $W$ and no spin accumulation. Horizontal arrows represent elastic spin scattering. (b) Elastically relaxed state. Elastic relaxation produces spin accumulation $\mu_{sz}$ from energy accumulation $W$. The full/half-filled/empty circles represent occupied/partially filled/unoccupied states. The effect depends on the asymmetry between spin-resolved density of states $N_\uparrow(\varepsilon)$ and $N_\downarrow(\varepsilon)$ and is therefore absent in the normal state.

to different energy levels. The resulting population imbalance can relax due to the elastic spin scattering process. As a result, all spin-up and spin-down states with identical energies become equally populated. As one can see from Fig. 2, in this state the net spin accumulation is nonzero because of the energy interval $\Delta - h_0 < E_p < \Delta + h_0$ where only the spin-down states exist [50].

The energy-to-spin conversion processes can be quantified using kinetic equations together with the collision integrals corresponding to the spin-orbit or spin-flip scattering. Introducing the distribution functions $f_{\uparrow/\downarrow}$ and densities of states $N_{\uparrow/\downarrow}$ in spin-up/down subbands, normalized to $N_\uparrow + N_\downarrow = 1$ in the normal state, we obtain [51] the spectral densities for spin and energy accumulations $f_s = N_\uparrow f_\uparrow - N_\downarrow f_\downarrow$ and $f_e = \varepsilon(N_\uparrow f_\uparrow + N_\downarrow f_\downarrow)$. The elastic spin-scattering collision integral is given by $\mathcal{I}_s = (f_s - \kappa_{se} f_e)/\mathcal{T}_1$, where $\mathcal{T}_1$ is the longitudinal spin relaxation time in the superconducting state [23] and spin-energy coupling coefficient $\kappa_{se}(\varepsilon) = (N_\uparrow - N_\downarrow)/[\varepsilon(N_\uparrow + N_\downarrow)]$. For weak spin splitting $h_0 \ll \Delta^2$, we can estimate $\kappa_{se} \sim h_0/(\varepsilon\Delta)$, where $\Delta$ is the superconducting gap.

The spin-diffusion equation modified by the spin-energy coupling is given by

$$\partial_x \mathcal{J}_{sz} = \frac{f_s(\varepsilon) - \kappa_{se} f_e}{\mathcal{T}_1}, \tag{2a}$$

$$\partial_x \mathcal{J}_e = I_{e-ph} + \Gamma f_e, \tag{2b}$$

where $\mathcal{J}_{sz}(\varepsilon)$ and $\mathcal{J}_e(\varepsilon)$ are the spectral densities of the time-independent spin $j_{sz} = \int d\varepsilon \mathcal{J}_{sz}$ and energy $j_e = \int d\varepsilon \mathcal{J}_e$ currents. The sources of these currents are determined by the boundary conditions at the FI interface with dynamical magnetization fixing the values of interfacial currents $\mathcal{J}_e(x=0) \propto \langle|\partial_t \boldsymbol{m}|^2\rangle$ and $\mathcal{J}_{sz}(x=0) \propto \boldsymbol{z}\cdot\langle \boldsymbol{m}\times\partial_t \boldsymbol{m}\rangle$. They are obtained generalizing the theory of normal-state spin battery effect [5] for the superconducting case [51]. In the limit of small SC film thickness $d$ the solution for spin accumulation $\mu_{sz} = (\boldsymbol{\mu}_s\cdot\boldsymbol{z})$ is $\mu_{sz} = -d^{-1}\int d\varepsilon(\Gamma^{-1}\kappa_{se}\mathcal{J}_e + \mathcal{T}_1\mathcal{J}_{sz})$. The first term has a large prefactor $\Gamma^{-1}$ and provides the possibility of spin signal enhancement by the parameter $\kappa_{se}/(\Gamma\mathcal{T}_1)$ as compared to the normal state, where only the second term contributes. The detailed calculation [51] described below shows that both $\mathcal{J}_e$ and $\mathcal{J}_{sz}$ are not dramatically smaller than their normal state magnitudes down to $T \approx 0.3T_c$. Thus $\mu_{sz}$ is enhanced by the factor $\kappa_{se}/(\Gamma\mathcal{T}_1)$ at $T/T_c \approx 0.8$–$0.9$.

In the limit of a short elastic mean-free path, the described effects are quantified using the Keldysh-Usadel equation [39,40]

$$-\{\hat{\tau}_3\partial_t\,\check{,}\,\check{g}\} + \partial_x(D\check{g}\circ\partial_x\check{g}) = [\Delta\hat{\tau}_1 + \check{\Gamma} + \check{\Sigma}_{so}\,\check{,}\,\check{g}] \tag{3}$$

for the quasiclassical Green's function (GF) $\check{g}$ in 8×8 space consisting of Keldysh, Nambu, and spin indices [23]. The diffusion constant is $D$, the elastic spin relaxation is determined by the spin-orbit scattering self-energy $\check{\Sigma}_{so} = \boldsymbol{\sigma}\cdot\check{g}\boldsymbol{\sigma}/(6\tau_{so})$ [51], while $\check{\Gamma}$ describes the coupling to the normal reservoir to model the *inelastic relaxation* [52].

The spin splitting and pumping induced by the electron scattering at the FI interface $x = 0$ are modelled by the *dynamical boundary conditions* [40,53]

$$D\check{g}\circ\partial_x\check{g}(x=0) = iJ_{sd}[\hat{\tau}_3\hat{\sigma}\mathbf{m}\,\check{,}\,\hat{g}]\,, \tag{4}$$

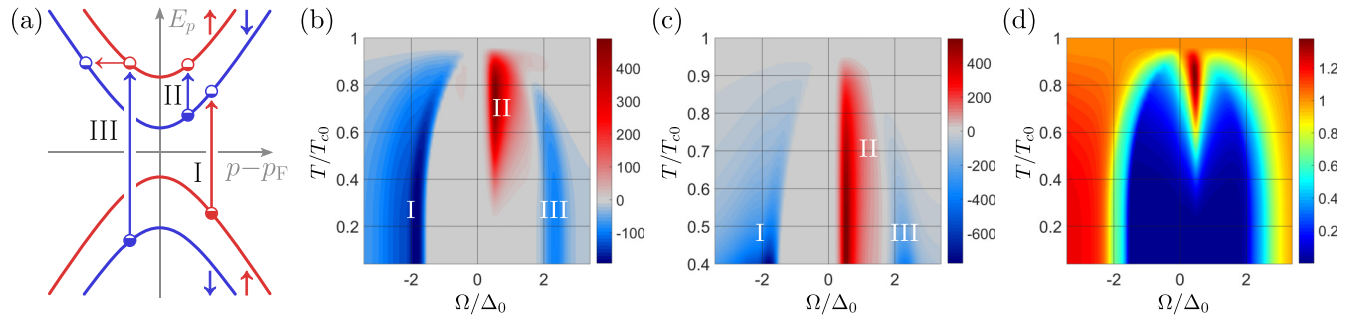


FIG. 3. (a) Quasiparticle excitation processes of the spin-split Bogoliubov spectrum. Vertical blue/red arrows are due to the absorption of a magnon with spin ±1. Horizontal arrows represent rapid spin relaxation. The filling of the circles shows the occupation of the states after spin relaxation. The corresponding peaks are labeled as I–III in the next panels. (b) Pumped spin accumulation $(T_{c0}/h_\Omega^2)\mu_z(T,\Omega)$, (c) nonlocal voltage $(eT_{c0}/h_\Omega^2)V_D(\Omega,T)$, and (d) pumped energy accumulation $W(T,\Omega)/W(T_c,\Omega)$, generated by the magnetization dynamics in the setup of Fig. 1. The parameters used for (b)–(d) are $\Gamma/T_{c0}=10^{-3}$, $h_0/T_{c0}=0.528$, and $\tau_{so}^{-1}/T_{c0}=1.19$. For these parameters $T_c\approx 0.9T_{c0}$, where $T_{c0}$ is the critical field at $h_0=\tau_{so}^{-1}=0$.

where we denote $[A\circ B](t_1,t_2)=\int dt A(t_1,t)B(t,t_2)-B(t_1,t)A(t,t_2)$ and similarly for the anticommutator $\{X\circ Y\}$. Here the interface is characterized by the effective exchange coupling [54] $J_{sd}$. Within the minimal model of the FI [53,55] it can also be expressed through the spin-mixing angle [39,40]. The longitudinal spin-relaxation time can be expressed in terms of the Green functions as $\mathcal{T}_1^{-1}=\frac{N_\uparrow+N_\downarrow}{6N_\uparrow N_\downarrow\tau_{so}}\mathrm{Tr}[(\hat g_s^{RA})^2-(\hat g_t^{RA})^2]$, where $\hat g_s^{RA}$ and $\hat g_t^{RA}$ are the singlet and triplet parts of $\hat g^R-\hat g^A=\hat g_s^{RA}+\hat g_t^{RA}$ [23].

We assume the time-dependent magnetization is $\boldsymbol{m}_\perp(t)=m_\Omega(\cos(\Omega t),\sin(\Omega t),0)$ consisting of the left- and right-hand parts $\boldsymbol{m}_\perp(t)=m_{\Omega,l}e^{i\Omega t}(\boldsymbol{x}-i\boldsymbol{y})+m_{-\Omega,r}e^{-i\Omega t}(\boldsymbol{x}+i\boldsymbol{y})$ with $m_{\Omega,l}=m_{-\Omega,r}=m_\Omega/2$. In general, solving Eqs. (3) and (4) to the second order in time-dependent field we obtain the stationary second-order correction to the Keldysh component of the GF $\hat g^K(\varepsilon)\propto m_\Omega^2$. It consists of corrections to the spectral function analogous to those induced by the electromagnetic irradiation [56,57] and of the anomalous part [58–61] $\hat g^a$ which determines the stationary spin accumulation and thereby the nonlocal voltage in Eq. (1). The calculation of $\hat g^a$ and its relation to the observables $W$, $\mu_{sz}$ and the distribution functions $f_\uparrow$, $f_\downarrow$ is presented in Supplemental Material [51]. It provides the general expression for the spin accumulation

$$\mu_{sz}(\Omega,T)=\chi_{lr}(\Omega,T)m_{l,\Omega}m_{r,-\Omega}, \tag{5}$$

where $\chi_{lr}$ is the second-order spin response function.

Here we consider a superconductor film with thickness $d_S\ll\ell_{sn},\xi_0$ small compared to the spin relaxation and coherence lengths in the superconductor. Then Eqs. (3) and (4) can be reduced [51] to the coordinate-independent Usadel equation with an effective Zeeman field $\boldsymbol{h}=J_{\rm sd}\boldsymbol{m}/d$ so that $h_0=J_{\rm sd}/d$ and $h_\Omega=h_0m_\Omega$.

The calculated dependencies of pumped spin accumulation $\mu_{sz}$, nonlocal voltage $V_D$, and energy $W$ are shown in Figs. 3(b)–3(d). One can see the clear correlation between these three quantities resulting from the strong spin-energy coupling in spin-split superconductors. The key feature of $\mu_{sz}(\Omega)$ and $V_D(\Omega)$ dependencies are the sharp peaks labeled by I and II as well as the less pronounced peak labeled by III corresponding to the different spin excitation processes shown schematically on the energy level diagram Fig. 3(a).

The excitation processes I and II create nonequilibrium quasiparticle states on the spin-down branch at the energy interval $\Delta-h_0<E_p<\Delta+h_0$, which corresponds to the situation with spin-energy accumulation shown in Fig. 2. Such states can relax only due to the slow energy relaxation which determines the large amplitude of the peaks I and II in Figs. 3(b) and 3(c). The size of these peaks scale as $\min(\tau_s,\Delta^{-1})h_0/(\tau_s\Gamma)$ as demonstrated by the series of plots for different parameters [51]. The process III is more complicated since it requires the existence of subgap spin-up states at $[\Delta-h_0,\Delta+h_0]$ energy interval which appear due to the broadening of spin subbands by the spin relaxation. The equilibration of spin-up and spin-down populations shown by the horizontal arrow leads to $f_\uparrow=f_\downarrow$ but the spin accumulation appears due to the DOS difference $N_\downarrow>N_\uparrow$.

Results in Figs. 3(b) and 3(c) predict sizable spin and voltage signals even for low frequencies $\Omega\ll\Delta_0$. They are especially pronounced near the peak II associated with electron paramagnetic resonance frequency $\Omega\approx 2h_0$ usually reached in FMR experiments with resonance frequencies around several GHz. The excitation process II in Fig. 3(a) polarizes existing quasiparticles and therefore disappears at low temperatures $T\ll T_c$. The processes I and III exist even at $T\to 0$ since they break Cooper pairs and create spin-polarized quasiparticles out from the vacuum state. As a result peaks I and III become exponentially diverging in the voltage signal at low temperatures $T\ll T_c$ [not shown in Fig. 3(c)], $V_D\propto e^{\Delta/T}$ since the local conductance $G_F\propto e^{-\Delta/T}$ in Eq. (1).

Because of energy conservation $W(\Omega)=\alpha(\Omega)\Omega^2m_\Omega^2/\Gamma$, where $\alpha(\Omega)$ is the frequency-dependent increase of Gilbert damping. The plot of the ratio $W(\Omega,T)/W(\Omega,T_c)=\alpha(\Omega,T)/\alpha(\Omega,T_c)$ shows the presence of the superconducting gap since the damping is generally suppressed for $\Omega<2\Delta_0$. For temperatures somewhat below $T_c$ there is a coherence peak [37–40] at around $\Omega\approx 2h_0$.

Next, we consider the spin accumulation driven by the stochastic magnetization corresponding to the *magnon thermal field* at temperature $T_m\neq T$ which can be controlled with the help of electrical spin injection based on the spin Hall effect [11,34]. For that we find $\mu_{sz}$ by averaging Eq. (5) over the fluctuations of magnetization. This can be done [51] by replacing the product of classical field components with the

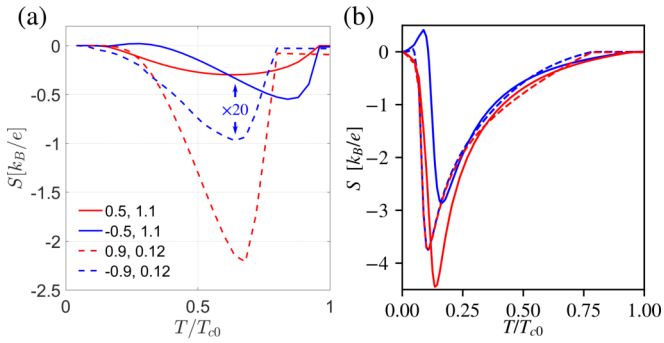


FIG. 4. Magnon Seebeck coefficient $S(T)$ in FI/SC/FM setup calculated using (a) model energy relaxation (3) with $\Gamma = 10^{-3}T_{c0}$ or (b) quasiequilibrium model (7) with electron-phonon relaxation. Red (blue) curves correspond to $(\boldsymbol{h}_0 \cdot \boldsymbol{m}_0) > (<)0$. Blue curves in (a) are multiplied by 20 for clarity. Solid and dashed lines are for $|h_0| = 0.5T_{c0}$, $\tau_{so}^{-1} = 1.1T_{c0}$ (Nb) and $|h_0| = 0.9T_{c0}$, $\tau_{so}^{-1} = 0.12T_{c0}$ (Al), respectively; $P_D = 0.5$, $\boldsymbol{P}_D \cdot \boldsymbol{h}_0 > 0$.

nonequilibrium Keldysh magnon propagator $m_{l,\Omega}m_{r,-\Omega} \to v_s\delta D^K(\Omega)$, where $v_s$ is the volume per spin, and summing over $\Omega$. In the stationary case $\delta D^K(\Omega) = D^{RA}(\Omega)\delta f_m(\Omega)$, where $D^{RA}(\Omega)$ and $f_m$ are the magnon density of states and the distribution function [51]. For the thermally biased magnon state $\delta f_m(\Omega) = n_B(\Omega/T_m) - n_B(\Omega/T)$, where $n_B(\Omega/T) = \coth(\Omega/2T)$. This approach generalizes the calculation of the magnon-driven spin current [38,62,63] to that of the magnon-driven spin accumulation.

For small magnon temperature bias this spin accumulation $\mu_{sz} \propto (T - T_m)$ and the detector voltage (1) can be expressed through the linear Seebeck coefficient characterizing the conversion of magnon temperature into the electric signal in FI/SC/FM nonlocal circuit $V_D = S(T - T_m)$

$$S = P_D v_s m_M^{3/2} \frac{G_{Fn}}{eG_F} \int_0^\infty \sqrt{\Omega}\chi_{lr}\partial_T n_B d\Omega, \tag{6}$$

where $v_s$, the volume per unit spin in FI, determines the number of magnon modes. For YIG [64], $m_M \approx 1\ \mathrm{eV}^{-1}\ \text{Å}^{-2}$ and [65] $v_s \approx 500\ \text{Å}^3$. Figure 4 shows $S(T)$ for parameters qualitatively corresponding to the EuS/Al and YIG/Nb based FI/SC bilayers that have been studied recently [34,49].

The spin signals are enhanced even more due to the energy dependence of the inelastic scattering rate when the relaxation is due to the electron-phonon coupling. This can be demonstrated in the quasiequilibrium limit, assuming the rapid internal thermalization process that allows us to parametrize the distribution function by temperature $T_S$ and the spin-dependent chemical potential shift $eV_s$. Then kinetic Eq. (2) can be written as the following system describing energy, spin, and charge currents at SC/FI and SC/FM interfaces

$$\begin{aligned} G_{e\text{-}ph}(T_S - T_{ph}) &= G_{me}(T_m - T_S) \\ \mathcal{V}_S \nu e V_s/\tau_{sa} &= G_{ms}(T_m - T_S) \\ (G_F/G_{Fn})V_D &= P_D V_s + \alpha_{th}(T_S - T_F). \end{aligned} \tag{7}$$

Here $G_{e\text{-}ph}$ is the electron-phonon thermal conductance, $\alpha_{th} = eP_D\int_0^\infty (N_\uparrow - N_\downarrow)\partial_T n_0 d\varepsilon$ is the thermoelectric coefficient at the SC/FM interface [20,21], $\mathcal{V}_S$ the superconductor volume, $\nu$ its density of states, and the energy-averaged spin relaxation rate is $\tau_{sa}^{-1} = \int_0^\infty d\varepsilon\,(\partial_\varepsilon n_0)\mathcal{T}_1^{-1}N_\uparrow N_\downarrow/(N_\uparrow + N_\downarrow)$. The magnon-electron conductances for spin and heat, $G_{ms}$ and $G_{me}$, are expressed [51] through the linear spin susceptibility [40,66] and were previously studied in the normal state [67,68]. Further we assume that the temperature of the phonon heat bath is equal to that of the ferromagnetic metal electrode $T_F = T_S$ to obtain the electric Seebeck coefficient

$$S = \frac{G_{Fn}}{G_F}\left(\frac{P_D\tau_{sa}G_{ms}}{\mathcal{V}_S\nu} + \frac{\alpha_{th}G_{me}}{G_{me} + G_{e\text{-}ph}}\right). \tag{8}$$

The second term is again due to the spin-energy mixing, and it provides the dominating contribution in the superconducting state. The Seebeck coefficient is plotted in Fig. 4(b) [69]. Compared to the full nonequilibrium case [Fig. 4(a)], we find that due to the rapid decrease of the electron-phonon coupling with decreasing temperature, the signal persists to lower temperatures and is mainly limited by the Seebeck coefficient of the SC/FM junction [21].

The large value of the Seebeck coefficient converting the magnon temperature difference to an electrical voltage indicates that this device can be used as an ultrasensitive detector of propagating magnons [51], analogous to the thermoelectric detector suggested in Refs. [70,71]. The detector can have a very low noise equivalent power of the order of $NEP^2 \sim G_{\text{th}}T^2$, limited by the weak thermal conductance $G_{\text{th}} = G_{me} + G_{e\text{-}ph}$ from the superconductor to the relevant heat baths. Similar to the other nanoscale superconducting detectors [72–74], they will also have a very good energy resolution $\Delta E = NEP\sqrt{\tau_{\text{eff}}}$, provided that the thermal relaxation time $\tau_{\text{eff}}$ is not too long. With suitable setting one can then approach even the detection of single propagating magnons with frequencies of a few tens of GHz.

To conclude we have shown how the electron-hole symmetry breaking present in SC/FI bilayers mixes the spin and energy modes and leads to a giant enhancement of the spin battery effect. This leads to the large magnon-driven Seebeck effect which can be considered as a very sensitive detector of magnons. We expect this effect also to explain the giant spin-Hall signal measured in Ref. [34], but its precise description would require appending the theory with the description of the spin-Hall angle [75–77].

The mechanism of producing giant spin signals does not necessarily require superconductors, but we expect similar effects in any system exhibiting strong spin-resolved electron-hole asymmetry, such as semimetals in the presence of large exchange fields or magnetic topological insulators [78]. Such systems allow for an electrical access to the energy dissipation processes in ferromagnetic resonance or detailed studies of the magnon spectra via the heat conductance $G_{me}$ between electrons and magnons.

We thank R. A. Duine for discussions. This work was supported by the Academy of Finland Projects 297439 and 317118, the European Union's Horizon 2020 Research and Innovation Framework Programme under Grant No. 800923 (SUPERTED), and Jenny and Antti Wihuri Foundation. The work of M.A.S. was supported by Russian Science Foundation (Grant No. 20-12-00053).

[1] S. Wolf, D. Awschalom, R. Buhrman, J. Daughton, v. S. von Molnár, M. Roukes, A. Y. Chtchelkanova, and D. Treger, Science **294**, 1488 (2001).

[2] I. Žutić, J. Fabian, and S. D. Sarma, Rev. Mod. Phys. **76**, 323 (2004).

[3] G. E. W. Bauer, E. Saitoh, and B. J. van Wees, Nat. Mater. **11**, 391 (2012).

[4] Y. Tserkovnyak, A. Brataas, and G. E. W. Bauer, Phys. Rev. Lett. **88**, 117601 (2002).

[5] A. Brataas, Y. Tserkovnyak, G. E. W. Bauer, and B. I. Halperin, Phys. Rev. B **66**, 060404(R) (2002).

[6] Y. Tserkovnyak, A. Brataas, G. E. W. Bauer, and B. I. Halperin, Rev. Mod. Phys. **77**, 1375 (2005).

[7] H. Nakayama, M. Althammer, Y.-T. Chen, K. Uchida, Y. Kajiwara, D. Kikuchi, T. Ohtani, S. Geprägs, M. Opel, S. Takahashi, R. Gross, G. E. W. Bauer, S. T. B. Goennenwein, and E. Saitoh, Phys. Rev. Lett. **110**, 206601 (2013).

[8] M. Weiler, M. Althammer, M. Schreier, J. Lotze, M. Pernpeintner, S. Meyer, H. Huebl, R. Gross, A. Kamra, J. Xiao, Y.-T. Chen, H. J. Jiao, G. E. W. Bauer, and S. T. B. Goennenwein, Phys. Rev. Lett. **111**, 176601 (2013).

[9] K. Uchida, J. Xiao, H. Adachi, J. Ohe, S. Takahashi, J. Ieda, T. Ota, Y. Kajiwara, H. Umezawa, H. Kawai, G. E. W. Bauer, S. Maekawa, and E. Saitoh, Nat. Mater. **9**, 894 (2010).

[10] A. Chumak, V. Vasyuchka, A. Serga, and B. Hillebrands, Nat. Phys. **11**, 453 (2015).

[11] L. Cornelissen, J. Liu, R. Duine, J. B. Youssef, and B. van Wees, Nat. Phys. **11**, 1022 (2015).

[12] H. Yang, S.-H. Yang, S. Takahashi, S. Maekawa, and S. S. Parkin, Nat. Mater. **9**, 586 (2010).

[13] C. Quay, D. Chevallier, C. Bena, and M. Aprili, Nat. Phys. **9**, 84 (2013).

[14] M. J. Wolf, F. Hübler, S. Kolenda, H. v. Löhneysen, and D. Beckmann, Phys. Rev. B **87**, 024517 (2013).

[15] F. Hübler, M. Wolf, D. Beckmann, and H. v. Löhneysen, Phys. Rev. Lett. **109**, 207001 (2012).

[16] S. Kolenda, C. Sürgers, G. Fischer, and D. Beckmann, Phys. Rev. B **95**, 224505 (2017).

[17] J. Heidrich and D. Beckmann, Phys. Rev. B **100**, 134501 (2019).

[18] J. Linder and J. W. Robinson, Nat. Phys. **11**, 307 (2015).

[19] W. Han, S. Maekawa, and X.-C. Xie, Nat. Mater. **19**, 139 (2020).

[20] F. S. Bergeret, M. Silaev, P. Virtanen, and T. T. Heikkilä, Rev. Mod. Phys. **90**, 041001 (2018).

[21] A. Ozaeta, P. Virtanen, F. S. Bergeret, and T. T. Heikkilä, Phys. Rev. Lett. **112**, 057001 (2014).

[22] M. Silaev, P. Virtanen, F. S. Bergeret, and T. T. Heikkilä, Phys. Rev. Lett. **114**, 167002 (2015).

[23] T. T. Heikkilä, M. Silaev, P. Virtanen, and F. S. Bergeret, Prog. Surf. Sci. **94**, 100540 (2019).

[24] T. Krishtop, M. Houzet, and J. S. Meyer, Phys. Rev. B **91**, 121407(R) (2015).

[25] I. V. Bobkova and A. Bobkov, JETP Lett. **101**, 118 (2015).

[26] I. V. Bobkova and A. M. Bobkov, Phys. Rev. B **96**, 104515 (2017).

[27] P. Virtanen, T. T. Heikkilä, and F. S. Bergeret, Phys. Rev. B **93**, 014512 (2016).

[28] M. Kuzmanović, B. Y. Wu, M. Weideneder, C. H. L. Quay, and M. Aprili, Nat. Commun. **11**, 4336 (2020).

[29] C. Bell, S. Milikisyants, M. Huber, and J. Aarts, Phys. Rev. Lett. **100**, 047002 (2008).

[30] T. Wakamura, H. Akaike, Y. Omori, Y. Niimi, S. Takahashi, A. Fujimaki, S. Maekawa, and Y. Otani, Nat. Mater. **14**, 675 (2015).

[31] K.-R. Jeon, C. Ciccarelli, A. J. Ferguson, H. Kurebayashi, L. F. Cohen, X. Montiel, M. Eschrig, J. W. A. Robinson, and M. G. Blamire, Nat. Mater. **17**, 499 (2018).

[32] K.-R. Jeon, X. Montiel, S. Komori, C. Ciccarelli, J. Haigh, H. Kurebayashi, L. F. Cohen, A. K. Chan, K. D. Stenning, C.-M. Lee, M. G. Blamire, and J. W. A. Robinson, Phys. Rev. X **10**, 031020 (2020).

[33] I. A. Golovchanskiy, N. N. Abramov, V. S. Stolyarov, V. I. Chichkov, M. Silaev, I. V. Shchetinin, A. A. Golubov, V. V. Ryazanov, A. V. Ustinov, and M. Y. Kupriyanov, Phys. Rev. Appl. **14**, 024086 (2020).

[34] K.-R. Jeon, J.-C. Jeon, X. Zhou, A. Migliorini, J. Yoon, and S. S. P. Parkin, ACS Nano **14**, 15874 (2020).

[35] A. Brataas and Y. Tserkovnyak, Phys. Rev. Lett. **93**, 087201 (2004).

[36] J. P. Morten, A. Brataas, G. E. W. Bauer, W. Belzig, and Y. Tserkovnyak, Europhys. Lett. **84**, 57008 (2008).

[37] M. Inoue, M. Ichioka, and H. Adachi, Phys. Rev. B **96**, 024414 (2017).

[38] T. Kato, Y. Ohnuma, M. Matsuo, J. Rech, T. Jonckheere, and T. Martin, Phys. Rev. B **99**, 144411 (2019).

[39] M. A. Silaev, Phys. Rev. B **102**, 180502(R) (2020).

[40] M. A. Silaev, Phys. Rev. B **102**, 144521 (2020).

[41] M. T. Ahari and Y. Tserkovnyak, Phys. Rev. B **103**, L100406 (2021).

[42] M. Trif and Y. Tserkovnyak, Phys. Rev. Lett. **111**, 087602 (2013).

[43] R. Ojajärvi, J. Manninen, T. T. Heikkilä, and P. Virtanen, Phys. Rev. B **101**, 115406 (2020).

[44] K.-R. Jeon, C. Ciccarelli, H. Kurebayashi, J. Wunderlich, L. F. Cohen, S. Komori, J. W. A. Robinson, and M. G. Blamire, Phys. Rev. Appl. **10**, 014029 (2018).

[45] E. Gershenzon, M. Gershenzon, G. Gol'tsman, A. Lyul'kin, A. Semenov, and A. Sergeev, Sov. Phys. JETP **70**, 505 (1990).

[46] T. M. Klapwijk, P. A. van der Plas, and J. E. Mooij, Phys. Rev. B **33**, 1474 (1986).

[47] A. Brataas, Y. Tserkovnyak, and G. E. W. Bauer, Phys. Rev. Lett. **101**, 037207 (2008).

[48] R. Meservey and P. Tedrow, Phys. Rep. **238**, 173 (1994).

[49] A. Hijano, S. Ilić, M. Rouco, C. G. Orellana, M. Ilyn, C. Rogero, P. Virtanen, T. Heikkilä, S. Khorshidian, M. Spies *et al.*, Phys. Rev. Research **3**, 023131 (2021).

[50] This picture is valid for weak spin relaxation with $\tau_s^{-1} \ll \Delta$. For larger $\tau_s^{-1}$ the spectrum becomes more complicated as the spin ceases to be a good quantum number. Our quasiclassical approach takes into account this spin mixing.

[51] See Supplemental Material at http://link.aps.org/supplemental/10.1103/PhysRevB.103.224524 for a derivation of the general relation between spin and energy currents generated by magnetization dynamics, a derivation of kinetic equations with spin-energy coupling and calculation of the anomalous parts of interfacial spin and energy currents, a derivation of the boundary conditions for Green's functions in the S/FI system with stochastic magnetization field, e.g., thermal magnons, a derivation of the second-order perturbation theory equations,

results of such calculations for various parameters, and the comparison with the nonperturbative numerical solution of the Keldysh-Usadel equation with a time-dependent Zeeman field, and estimates for the figures of merit of the magnon detector. The Supplemental cites Refs. [79–81].

[52] H. T. Simensen, L. G. Johnsen, J. Linder, and A. Brataas, Phys. Rev. B **103**, 024524 (2021).

[53] T. Tokuyasu, J. A. Sauls, and D. Rainer, Phys. Rev. B **38**, 8823 (1988).

[54] Y. Ohnuma, H. Adachi, E. Saitoh, and S. Maekawa, Phys. Rev. B **89**, 174417 (2014).

[55] A. Millis, D. Rainer, and J. A. Sauls, Phys. Rev. B **38**, 4504 (1988).

[56] A. V. Semenov, I. A. Devyatov, P. J. de Visser, and T. M. Klapwijk, Phys. Rev. Lett. **117**, 047002 (2016).

[57] J. Linder, M. Amundsen, and J. A. Ouassou, Sci. Rep. **6**, 38739 (2016).

[58] G. M. Eliashberg, Zh. Eksp. Teor. Fiz. **61**, 1254 (1971).

[59] L. P. Gor'kov and N. B. Kopnin, Sov. Phys. Usp. **18**, 496 (1975).

[60] A. Larkin and Y. Ovchinnikov, Zh. Eksp. Teor. Fiz. **73**, 299 (1977).

[61] S. N. Artemenko and A. Volkov, Sov. Phys. Usp. **22**, 295 (1979).

[62] H. Adachi, J.-I. Ohe, S. Takahashi, and S. Maekawa, Phys. Rev. B **83**, 094410 (2011).

[63] H. Adachi, K.-I. Uchida, E. Saitoh, and S. Maekawa, Rep. Prog. Phys. **76**, 036501 (2013).

[64] C. M. Srivastava and R. Aiyar, J. Phys. C **20**, 1119 (1987).

[65] V. Cherepanov, I. Kolokolov, and V. L'vov, Phys. Rep. **229**, 81 (1993).

[66] K. Maki, Phys. Rev. B **8**, 191 (1973).

[67] S. A. Bender and Y. Tserkovnyak, Phys. Rev. B **91**, 140402(R) (2015).

[68] L. J. Cornelissen, K. J. H. Peters, G. E. W. Bauer, R. A. Duine, and B. J. van Wees, Phys. Rev. B **94**, 014412 (2016).

[69] Figure 4 assumes for simplicity that the electron-phonon coupling in Nb is the same as in Al.

[70] T. T. Heikkilä, R. Ojajärvi, I. J. Maasilta, E. Strambini, F. Giazotto, and F. S. Bergeret, Phys. Rev. Appl. **10**, 034053 (2018).

[71] S. Chakraborty and T. T. Heikkilä, J. Appl. Phys. **124**, 123902 (2018).

[72] J. Govenius, R. E. Lake, K. Y. Tan, V. Pietilä, J. K. Julin, I. J. Maasilta, P. Virtanen, and M. Möttönen, Phys. Rev. B **90**, 064505 (2014).

[73] J. Govenius, R. E. Lake, K. Y. Tan, and M. Möttönen, Phys. Rev. Lett. **117**, 030802 (2016).

[74] R. Kokkoniemi, J. Govenius, V. Vesterinen, R. E. Lake, A. M. Gunyhó, K. Y. Tan, S. Simbierowicz, L. Grönberg, J. Lehtinen, M. Prunnila *et al.*, Commun. Phys. **2**, 124 (2019).

[75] F. S. Bergeret and I. V. Tokatly, Phys. Rev. B **94**, 180502(R) (2016).

[76] I. V. Tokatly, Phys. Rev. B **96**, 060502(R) (2017).

[77] C. Huang, I. V. Tokatly, and F. S. Bergeret, Phys. Rev. B **98**, 144515 (2018).

[78] M. M. Otrokov, I. I. Klimovskikh, H. Bentmann, D. Estyunin, A. Zeugner, Z. S. Aliev, S. Gaß, A. Wolter, A. Koroleva, A. M. Shikin *et al.*, Nature (London) **576**, 416 (2019).

[79] R. C. Dynes, J. P. Garno, G. B. Hertel, and T. P. Orlando, Phys. Rev. Lett. **53**, 2437 (1984).

[80] A. Abrikosov and L. Gor'kov, Sov. Phys. JETP **15**, 752 (1962).

[81] A. Kamenev, *Field Theory of Non-Equilibrium Systems* (Cambridge University Press, Cambridge, 2011).